ELSEVIER

Solvable chaos

B. Grammaticos [a], A. Ramani [b], C.M. Viallet [c,*]

[a] *GMPIB, Université Paris VII, Tour 24-14, 5e étage, case 7 021, F-75251 Paris cedex 05, France*
[b] *Centre de Physique Théorique, UMR 7644 Ecole Polytechnique, F-91128 Palaiseau, France*
[c] *Laboratoire de Physique Théorique et des Hautes Energies, 4 Place Jussieu, Boite 126, F-75252 Paris cedex 05, France*

Abstract

We present classes of discrete reversible systems which are at the same time chaotic and solvable.
© 2005 Elsevier B.V. All rights reserved.

1. Introduction

Chaos and solvability are antithetical notions and their coexistence in a dynamical system may sound paradoxical. The term chaos is traditionally used to designate systems which exhibit crucial dependence on the initial conditions manifested through exponentially diverging trajectories and extreme instability [1]. On the other hand, solvability is often associated to smooth, regular behavior, related to the existence of invariants, and is usually coming from integrability.

In what follows we shall show that the explicit solvability of a mapping is not incompatible with a chaotic behavior. This is done in the same spirit as in [2,3]

(see also [4]) but we will give example of reversible systems (i.e., there exists a similarity transformation between the forward evolution and the backward evolution), exhibiting at the same time features of chaos (e.g., sensitive dependence on the initial conditions, positive algebraic entropy, ergodicity), and which are solvable. Our point is neither to recall the possible coexistence of KAM tori and chaotic regions which is well known [5], nor to give the ultimate definition of integrability, solvability or chaos.

We aim to present reversible systems which lie on the border of solvability/integrability and chaos.

2. Specific examples

We will use maps which are constructed from recurrences, that is to say sequences where each term is

* Corresponding author.
 E-mail addresses: grammati@paris7.jussieu.fr
(B. Grammaticos), ramani@cpht.polytechnique.fr (A. Ramani),
viallet@lpthe.jussieu.fr (C.M. Viallet).

given as a function of the previous ones:

$$x_{n+1} = f(x_n, x_{n-1}, \ldots, x_{n-\nu}). \tag{1}$$

If x_{n+1} is a function of only x_n, we have a one-dimensional map, also called a system of order one. If $\nu = 1$ (respectively $\nu = r$) we may define from (1) a map in two dimensions (respectively $r + 1$ dimensions) by

$$[x_n, x_{n-1}, \ldots, x_{n-\nu}] \to [x_{n+1}, x_n, \ldots, x_{n-\nu+1}]. \tag{2}$$

The space of initial conditions is of dimension $\nu + 1$.

2.1. One-dimensional maps

We start with a well-known one-dimensional example to illustrate the fact that solvability is compatible with chaotic behavior:

$$x_{n+1} = 2x_n^2 - 1. \tag{3}$$

This map is know to be chaotic [6]. Using the similarity between (3) and the doubling rule for cosine: $\cos(2\omega) = 2\cos^2 \omega - 1$, the solution of (3) is given by $x_n = \cos 2^n \alpha$ where α is some constant determined by the initial conditions. We shall not dwell upon the exponentially fast loss of the memory of the initial conditions due to the presence of the 2^n factor: the existing literature covers the topic in an exhaustive way [1]. It remains that we have here an example of a system that is explicitly solvable and which has a chaotic behavior.

The previous example is not an isolated occurrence. Whole families of first-order (one-dimensional) systems exist which are solvable while at the same time exhibiting exponentially fast loss of the memory of the initial conditions. There exist a number of results in this direction for maps of the interval [2,3,7]. It was shown that the only nonlinear polynomial maps where the solution can be explicitly given are the map $x_{n+1} = x_n^2$ and (3), up to a homographic transformation.

For rational maps there exists a classification based on results of Ritt [8]. For degree one, the only solution is the homographic map. For degree 2, there exist 8 different recurrences, the simplest ones being

$$x_{n+1} = \frac{1}{2i}\left(x_n - \frac{1}{x_n}\right), \tag{4}$$

$$x_{n+1} = -\frac{1}{4}\left(x_n - 2 + \frac{1}{x_n}\right). \tag{5}$$

Their solutions can be given in terms of the Weierstraß elliptic function $\wp(z)$, defined through the equation $(\wp')^2 = 4\wp^3 - 4\wp$. Eq. (4) has solution $x_n = \wp((1 + i)^n z)$. Similarly the solution of (5) is $x_n = \wp^2((1 + i)^n z)$, and so on.

The major problem with the above mappings is that they are not invertible. While one can define the image of a given point in an unambiguous way, the same is not true for the inverse evolution. Moreover the number of preimages of a point grows exponentially fast (a property which was deemed incompatible with integrability [9]). In the next paragraph we will exhibit *reversible* maps, defined by birational transformations showing features of chaos and which are solvable. One condition to construct such maps is to consider transformations in more than one dimension.

2.2. Two-dimensional maps

In the case of transformation (3), the key ingredient was the doubling relation $\omega_{n+1} = 2\omega_n$ (or a higher multiple $\omega_{n+1} = k\omega_n$). We start from a linear equation:

$$\omega_{n+1} + \omega_{n-1} = k\omega_n. \tag{6}$$

The solution of (6) is straightforward: $\omega_n = a\lambda_+^n + b\lambda_-^n$ where $\lambda_\pm = (k \pm \sqrt{k^2 - 4})/2$. Exponentiating (6) and setting $x = e^\omega$ we obtain the recurrence:

$$x_{n+1}x_{n-1} = x_n^k. \tag{7}$$

The chaotic character of this map (for $k > 2$) can be assessed easily through the computation of its algebraic entropy [10]. This quantity is a measure of the complexity of the map and is given by $\epsilon = \lim_{n\to\infty} \log(d_n)/n$ where d_n is the degree of the nth iterate. In the case at hand we find that $\epsilon = \log(\lambda_+)$. This leads to $\epsilon > 0$ for $k > 2$. In fact the same value for the entropy is obtained for all the maps derived from (6).

While map (7) is rather trivial, it is possible to construct a much more interesting one by setting

$$x_n = \tan\omega_n. \tag{8}$$

We get the recurrence:

$$\frac{x_{n+1} + x_{n-1}}{1 - x_{n+1}x_{n-1}} = f_k(x_n), \tag{9}$$

where f_k is a rational function of x_n depending on the value of k. It is simply the expression of $\tan k\omega_n$ in terms of $\tan \omega_n \equiv x_n$. For the first few values of k we have $f_1(x_n) = x_n$, $f_2(x_n) = 2x_n/(1 - x_n^2)$, $f_3(x_n) = (3x_n - x_n^3)/(1 - 3x_n^2)$ etc. The case $k = 1$ corresponds to a trivial map which is periodic with period 3. The case $k = 2$ can be easily integrated. There exists an invariant $c = (x_{n-1} - x_n)/(1 + x_{n-1}x_n)$, which allows to reduce the map to a homographic one and solve it completely.

The case $k = 3$ is more interesting. Indeed the map constructed from the recurrence

$$x_{n+1} = \frac{3x_n - x_n^3 - x_{n-1}(1 - 3x_n^2)}{1 - 3x_n^2 + (3x_n - x_n^3)\,x_{n-1}} \tag{10}$$

is both chaotic and solvable (since it is linearizable). The generating function of the sequence of degrees [11] may easily be inferred from the first terms of this sequence:

$$g = \frac{1 + 2s + s^2 - 2s^3 + s^4 - 2s^5}{(1 - s)(1 + s + s^2)(1 - 3s + s^2)}. \tag{11}$$

The value of the algebraic entropy $\epsilon = \log((3 + \sqrt{5})/2)$ is read off from (11). This positive entropy is a sign of chaotic behavior.

Similar maps can be constructed for $k \geqslant 3$. They will have a positive algebraic entropy and be linearizable.

3. Graphical analysis

Fig. 1 shows the orbit of an arbitrary initial point under 10^6 iterations of the evolution (10), plotting the pairs (x_n, x_{n+1}) in the two-dimensional plane. It shows that the orbits tend to fill phase space.
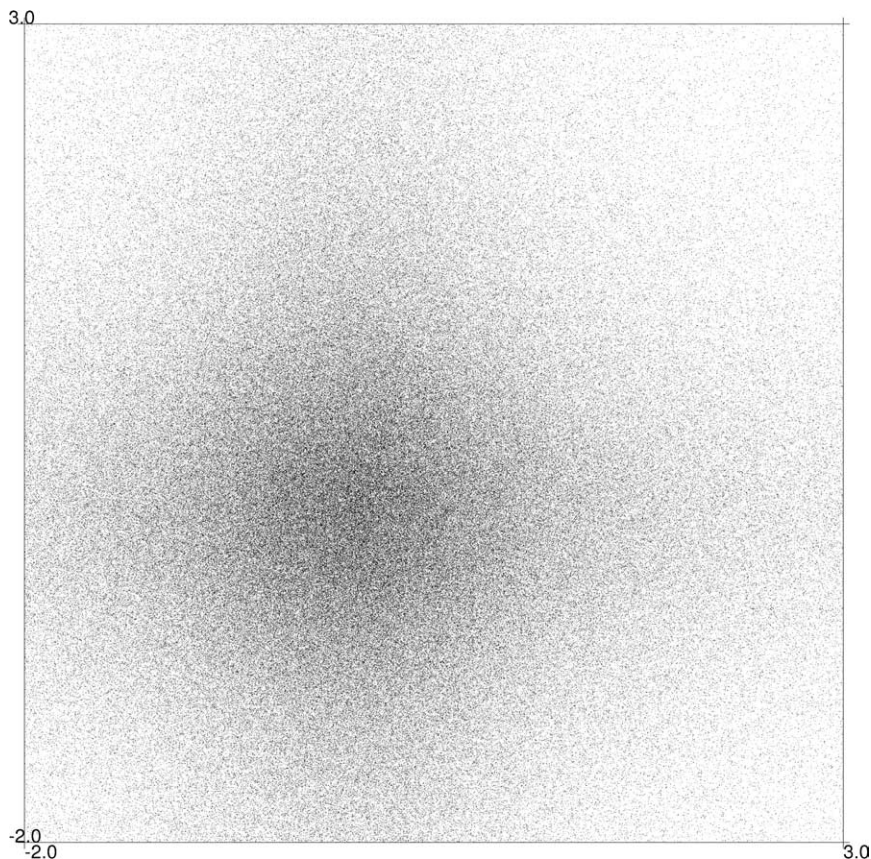

Fig. 1. A typical orbit of a point under map (10).

Fig. 2 shows the images of a segment under a dozen of iterations of (10). Pushing the iteration further does not change the qualitative features of the image. It just increases the density of lines.

The fact that the map (10) has an algebraic entropy of $\log((3 + \sqrt{5})/2)$ invites us to compare it to the map described in [12], which has the same algebraic entropy, and is chaotic:

$$x_{n+1} + x_{n-1} = x_n + \frac{a}{x_n^2} \qquad (12)$$

with a a constant.

The typical orbit of an arbitrary point was shown in [12], presenting large chaotic regions, and we do not reproduce it here.

Fig. 3 shows the images of a segment of a straight line under 27 iterations of (12), and is to be compared with Fig. 2. The overall pictures differ qualitatively.

A detailed analysis of the behavior of the iterates shows that in the case of the map (12) the evolution is slow till the points get near one of the singularities, in which case they get a major boost, which results in the rich structure of Fig. 3. On the contrary, in the case of map (10) neighboring points are uniformly repelled and the overall results are regular and smooth. Both have a strong dependence on the initial conditions, but in different ways.

All numerical calculations leading to Figs. 2 and 3 have been performed with multi-precision [13] arithmetics so as to guarantee the reliability of the results, and a test was performed on all image points: after an evolution of N steps, we "go back in time" the same number of steps to recover the initial data. We adjusted the precision in such a way that the true initial data and the result of this round trip did not differ by more than 10^{-3}.
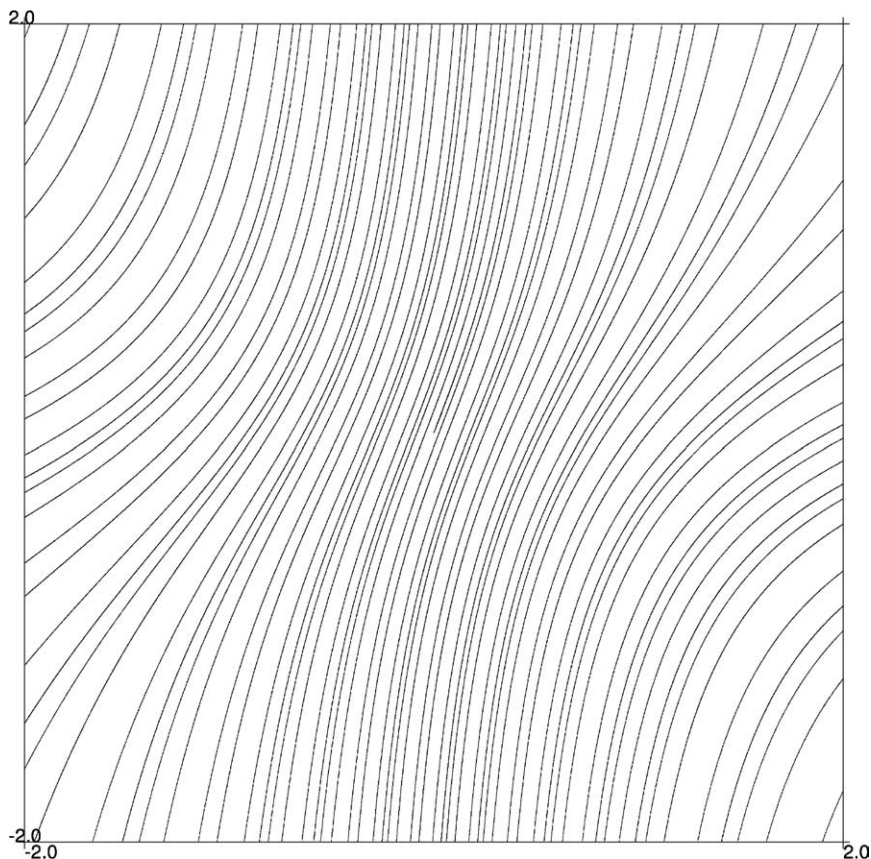

Fig. 2. Images of a segment under map (10).

The distinguishing feature of (10) compared to (12) if that (6) has an integral

$$(\omega_{n+1} - \lambda_+ \omega_n)(\omega_{n+1} - \lambda_- \omega_n) = cst \qquad (13)$$

with $\lambda_\pm = (3 \pm \sqrt{5})/2$. The ω-plane is foliated by invariant curves, but the picture is scrambled by the transformation (8) since the tangent function is periodic. It is easy to understand the aspect of Fig. 1. The curve (13) is transformed by (8) into

$$(\arctan x_{n+1} - \lambda_+ \arctan x_n)$$
$$\times (\arctan x_{n+1} - \lambda_- \arctan x_n) = \kappa \qquad (14)$$

with x_{n+1} and x_n the two coordinates of the plane of Fig. 1, and κ a constant. Such a curve cuts a line $x_n = \xi$ at an infinite dense set of points.

One may notice that there exist two holomorphic foliations which are left invariant by (9), as in the analysis of [14], and our construction exemplifies their result.

One interesting feature of transformation (8) is that it is not a mere change of coordinates. It takes a birational map into a birational one, changing the algebraic entropy.

4. Arithmetical analysis

The difference between maps (10) and (12) can be illustrated by an analysis based on the approach recently introduced by Roberts and Vivaldi [15]. These authors have studied the effect of the existence of rational integrals of motion for rational maps when the evolution is considered over a finite field. The simplest realization of such an evolution is through integer arithmetics modulo some prime integer p. The basic
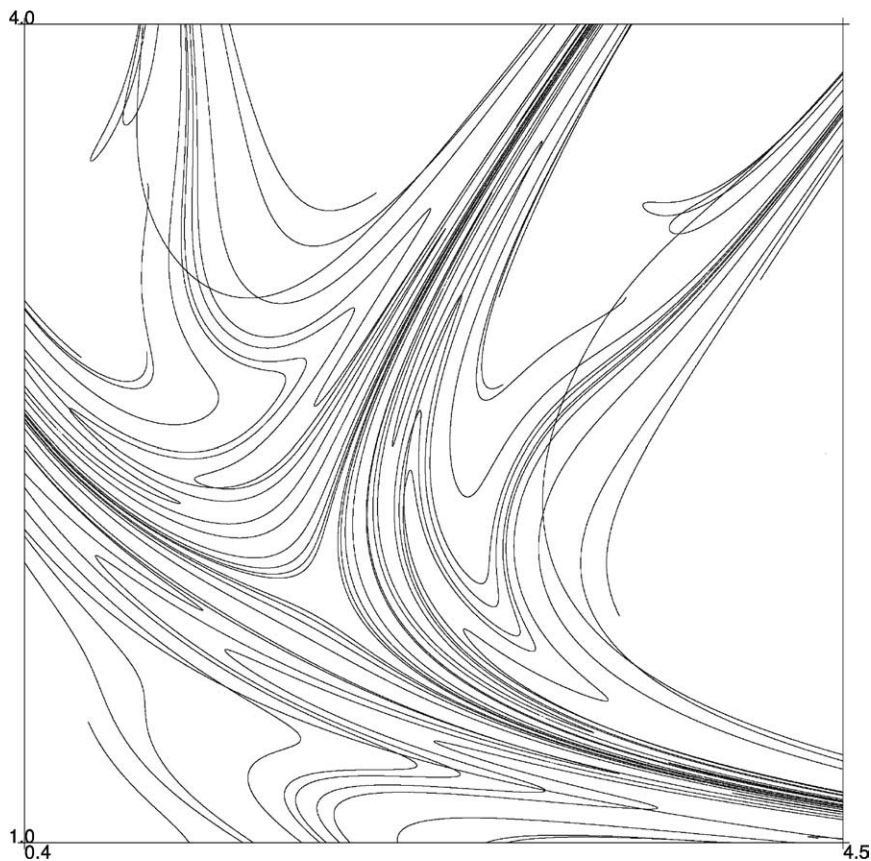

Fig. 3. Images of a segment under map (12).

observation of [15] (see also [16]) is that if there exists a rational invariant, the orbit is confined to an algebraic curve, and the genus g of this curve is at most one, if the original map is of infinite order. Such curves over finite fields have a maximum number of points (the Hasse–Weil bound $HW(p, g) = p + 1 + 2g\sqrt{p}$), and as a consequence the number of points on the same orbit is also bounded by $HW(p, g)$. In short: algebraically integrable maps have a large number of orbits and those are short. Chaotic maps have a smaller number of orbits and they are longer. Notice that this fits with the idea that chaotic orbits may explore the whole phase space, contrary to what happens in the integrable case.

We have performed a sampling of initial points for increasing values of p and plotted the mean value of the length of orbits (with the rule to terminate the iteration when meeting a singular point or closing a loop), for the maps (10), (12), and one additional map which is known to be algebraically integrable (so-called McMillan map), given by the recurrence:

$$x_{n+1} + x_{n-1} = 2a\frac{x_n}{x_n^2 - 1} \tag{15}$$

with a a free parameter.

Fig. 4 shows the values of the mean length for increasing p, normalized by dividing by $HW(p, 1) = p + 1 + 2\sqrt{p}$, for maps (10), (12), and (15). It discriminates between (10) and (12) by showing that the former verifies a virtual Hasse–Weil bound while the
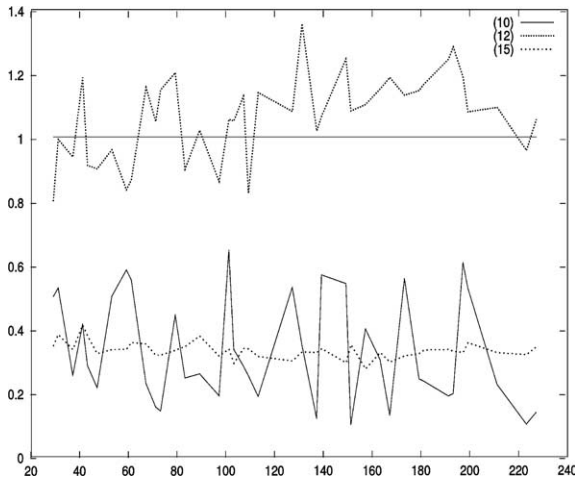

Fig. 4. Mean length of orbits vs. p.

latter does not. The curve corresponding to map (15) is there for reference, as well as the line corresponding to a constant normalized length of 1. Clearly, although the orbits are not confined to any invariant algebraic curve, the arithmetic test of [15] places the map (10) in the integrable class together with (15), in contrast to (12).

A more detailed analysis of the statistics of the length of orbits will be done elsewhere.

5. Generalizations

We can construct generalizations of (9), based on the properties of elliptic functions. Introduce $x_n = \wp(\omega_n)$ and $y_n = \wp'(\omega_n)$ where $\wp$ is the Weierstraß elliptic function with elliptic invariants g_2 and g_3. The addition formulae for the Weierstraß elliptic function yield:

$$x_{n+1} = \frac{1}{4}\left(\frac{h_k(x_n, y_n) + y_{n-1}}{f_k(x_n, y_n) - x_{n-1}}\right)^2 - f_k(x_n, y_n) - x_{n-1},$$

$$y_{n+1} = \frac{x_{n+1}(h_k(x_n, y_n) + y_{n-1})}{x_{n-1} - f_k(x_n, y_n)}$$
$$- \frac{f_k(x_n, y_n)y_{n-1} + h_k(x_n, y_n)x_{n-1}}{x_{n-1} - f_k(x_n, y_n)}, \tag{16}$$

where the functions f_k and h_k are the expressions of $\wp(k\omega_n)$ and $\wp'(k\omega_n)$ in terms of $x_n = \wp(\omega_n)$ and $y_n = \wp'(\omega_n)$.

We have to ensure that both (x_n, y_n) and x_{n-1}, y_{n-1} lie on the same elliptic curve, i.e.

$$y_n^2 = 4x_n^3 - g_2 x_n - g_3, \tag{17}$$
$$y_{n-1}^2 = 4x_{n-1}^3 - g_2 x_{n-1} - g_3. \tag{18}$$

Eqs. (17), (18) together with the formula for the duplication, triplication,... of the arguments yield the value of the f_k and h_k. Iteration (16) defines a map in four variables which has two algebraic invariants given by solving (17), (18) in terms of g_2, g_3:

$$g_2 = \frac{y_{n-1}^2 - y_n^2}{x_n - x_{n-1}} + 4\left(x_{n-1}^2 + x_n x_{n-1} + x_n^2\right), \tag{19}$$

$$g_3 = \frac{x_{n-1}y_n^2 - x_n y_{n-1}^2}{x_n - x_{n-1}} - 4x_n x_{n-1}(x_{n-1} + x_n). \tag{20}$$

For $k = 2$ we have $f_2 = -2x + z^2/(4y^2)$ and $h_2 = -y + 3xz/y - z^3/(4y^3)$ where z stands for $\wp''(\omega_n) =$

$6\wp^2(\omega_n) - g_2/2 \equiv 6x^2 - g_2/2$. In this case there exists an additional invariant

$$C = \left(\frac{y_{n-1} + y_n}{x_n - x_{n-1}}\right)^2 - 4(x_n + x_{n-1}) \tag{21}$$

and the map is integrable with vanishing entropy (quadratic growth of the degree).

For $k = 3$ we have $f_3 = x + 4y^2(12xy^2z - 4y^4 - z^3)/(12xy^2 - z^2)^2$ and $h_3 = -y - 4y(12xy^2z - 8y^4 - z^3)(12xy^2z - 4y^4 - z^3)/(12xy^2 - z^2)^3$. This case, and actually all cases with $k \geqslant 3$, have positive entropy and solvability is ensured through the relation to (6).

6. Conclusion

We have shown that there exist infinite families of rational maps which, at the same time, have positive algebraic entropy, present features of chaos, and are solvable. Their solvability is related to a reduction to a linear equation through the appropriate non rational transformations, but they remain reversible.

While the examples we exhibited here are based on specific Ansätze, there exist infinite families of solvable mappings with positive algebraic entropy. As a matter of fact one could perform the same derivation using any function for which one can express $f(x + y)$ in terms of $f(x)$ and $f(y)$.

Open questions remain, like what is the meaning of the statistics of the length of orbits in the arithmetic approach of [15,16]. We will return to that in some future publication.

References

[1] J.-P. Eckmann, D. Ruelle, Rev. Mod. Phys. 57 (3) (1985) 617.
[2] K. Umeno, Phys. Rev. E 55 (5) (1997) 5280.
[3] K. Umeno, Sūrikaisekikenkyūsho Kōkyūroku 1098 (1999) 104, chao-dyn/9704007.
[4] R.B. Potts, Bull. Austral. Math. Soc. 35 (1) (1987) 43.
[5] J.A.G. Roberts, G.R.W. Quispel, Phys. Rep. 216 (2–3) (1992) 63.
[6] P. Collet, J.-P. Eckmann, Iterated Maps on the Interval as Dynamical Systems, Progress in Physics, vol. 1, Birkhäuser, Boston, MA, 1980.
[7] A.P. Veselov, What is an integrable mapping, in: V.E. Zakharov (Ed.), What is Integrability, Springer-Verlag, Berlin, 1991, p. 251.
[8] J. Ritt, Trans. Amer. Math. Soc. 25 (1923) 399.
[9] B. Grammaticos, A. Ramani, K.M. Tamizhmani, J. Phys. A (27) (1994) 559.
[10] M. Bellon, C.-M. Viallet, Commun. Math. Phys. 204 (1999) 425.
[11] G. Falqui, C.-M. Viallet, Commun. Math. Phys. 154 (1993) 111.
[12] J. Hietarinta, C.-M. Viallet, Phys. Rev. Lett. 81 (2) (1998) 325.
[13] Gnu MultiPrecision, Arbitrary precision arithmetics software, see http://www.swox.com/gmp/.
[14] S. Cantat, C. Favre, J. Reine Angew. Math. 561 (2003) 199, math.CV/0206209.
[15] J.A.G. Roberts, F. Vivaldi, Phys. Rev. Lett. 90 (2003) 034102.
[16] J.A.G. Roberts, D. Jogia, F. Vivaldi, J. Nonlinear Math. Phys. 10 (Suppl. 2) (2003) 166.